Struct Multidisc Optim (2005) 29: 477–487
DOI 10.1007/s00158-004-0489-6

RESEARCH PAPER

C.W. King · M.I. Campbell · J.J. Beaman · S.V. Sreenivasan

# Synthesis of multistable equilibrium linkage systems using an optimization approach

Received: 16 June 2003 / Revised manuscript received: 30 April 2003, 11 August 2003, 24 August 2004 / Published online: 7 January 2005


**Abstract** This paper introduces a methodology for designing multistable equilibrium (MSE) systems. The methodology derives design criteria that relate system equilibrium characteristics to a potential energy curve. These design criteria are then used in a performance index that guides a candidate's potential energy to approach the desired potential energy curve. As an example, a four-bar linkage with linear translational springs attached demonstrates the design methodology and the difficulties inherent in synthesizing MSE systems. To solve for the unknown design variables of the example problem a genetic algorithm is used.

**Keywords** Equilibrium · Four-bar linkage · Multistable

## 1 Introduction

Often engineering systems are designed with optimized lengths, materials, and various other parameters such that the systems achieve high efficiency or performance for one specific equilibrium operating point. Thus, to operate far from the operating point, the actuation and control system can become unduly complicated and power intensive. The idea of multistable equilibrium (MSE) systems is that a passive subsystem is integrated to provide versatility in function, while actuation stays simple. Here, MSE systems are those that have more than one stable equilibrium configuration in which they can reside with no power input. Each stable configuration of the system is defined when its potential energy is at a local minimum.

The goal of MSE structures is to create a wide range of operating regimes for existing and novel mechanical systems, but without undue power consumption. Each equilibrium operating regime of an MSE system can be characterized by one or more of the following traits: position/shape, stiffness/natural frequency, and energy change between equilibria. Whether or not one needs to be concerned with the different design aspects is up to the designer of the system.

In this paper we use optimization methods to find solutions to problems that are not easily solved by human designers because the multimodal and bifurcative nature of MSE systems are highly nonintuitive. MSE systems require more strict synthesis tools such as those addressed in this paper. One underlying assumption is that all nonlinear devices or motions in a given system are sufficiently smooth. For instance, nonlinearities such as gear backlash and stiction are currently not addressed under the proposed methodology.

The proposed design synthesis methodology presents the user with a way to interpret engineering factors into a mathematical form that can be easily used for design and numerical optimization. The mathematical basis of the proposed design methodology focuses on how to properly shape the potential energy curve of the MSE system to match a desired energy curve. This desired energy curve is characterized by local descriptions about the equilibrium points. A mapping method is also introduced to help visualize what kinds of MSE system solutions are possible. This enables the designer to pick reasonable characteristics to describe the desired energy curve.

The subsequent literature review shows that there is substantial interest in the design of MSE systems, and in particular bistable systems and mechanisms. It is not the purpose of the proposed design methodology to explain why one would want to create an MSE system, but only how one can design an MSE system. Assuming the purpose of designing an MSE system is resolved beforehand, the designer should then pinpoint the important characteristics of the MSE system. Desired engineering characteristics then relate to specific mathematical constructions, such as maxima and minima within the potential energy curve of the system.

* Formerly associated with The University of Texas at Austin

C.W. King (✉)*
Uni-Pixel Displays, Inc.
E-mail: cking@uni-pixel.com

M.I. Campbell · J.J. Beaman · S.V. Sreenivasan
Department of Mechanical Engineering, The University of Texas at Austin, 1 University Station, #C2200, Austin, TX 78712, USA
E-mail: mc1@mail.utexas.edu

As a hypothetical example problem suitable for using the proposed design methodology imagine the design of a flexible robotic fish that in one configuration is characterized by a tuna-like shape of high tail-beat frequency for efficient long-range swimming, and another equilibrium is characterized by a long, slender, eel-shaped body with low stiffness for high mobility and agility. Although the function of the fish robot is always to swim, the different stable configurations are required to take advantage of the entirely different physical principles involved for each mode of swimming.

Another MSE system could be a sensor with multiple stiffnesses that allows for different resolution and range combinations enabling more accurate and versatile data acquisition. Thus, the 'shape' of this MSE sensor could be quite meaningless. As these two examples show, deciding on the important design criteria of an MSE system is problem dependent, and it is entirely up to the design engineer to choose correctly.

### 1.1 Literature review

Most of the existing literature on MSE systems is about bistable structures (Capanu et al. 2000; Howell et al. 1994; Opdahl et al. 1998). The discussion usually centers on the analysis of equilibrium positions rather than synthesis, although Schulze (1955) performed early work in synthesizing actuation force for a simple bistable design. Hafez et al. (2002) describe how to use many bistable devices in tandem to create an overall system with multiple configurations. The term 'bistable' is often used quite liberally as many of the design examples of bistable structures quoted in the literature are often not truly bistable at all in the sense of energy being at a minimum. Some are bistable in the sense of not requiring power input to maintain position, but they rely on interference fits, clamps, and friction to provide the two stable positions (Chironis 1991; Hoffman et al. 1999). Thus, these stable positions could be better characterized by hard kinematic constraints rather than minima in energy. These hard kinematic constraints often severely hamper the ability to create more stable equilibrium positions and allow for dynamic movement at each equilibrium configuration.

Much of the bistable literature mentions designing structures on the microelectromechanical systems (MEMS) level. Because of the dominance of surface friction forces inherent at the micro scale, many MEMS devices cannot use hinges. Thus, they rely on compliance to allow motion, and one must account for their elastic strain energy (Jensen and Howell 2000; Jensen et al. 1998; Saif 2000). One design by Capanu et al. (2000) uses simple electromagnetic actuation to move a valve from open to closed, and vice versa, while a permanent magnet keeps the valve open and elastic energy keeps it closed. Hafez et al. (2002) design a reconfigurable robotic arm based on similar physical principles. Many designs incorporating bistability use the concept of buckling (Schomburg and Goll 1998; Vangbo and Bäcklund 1998). Saif (2000) presents an extensive analysis of a buckled beam used as a bistable device while discussing the ability to tune the threshold force that moves the beam from one buckled state to the other.

Jensen and Howell (2000) establish a theory to guarantee bistable behavior in a certain class of compliant structures, but the theory treats each energy storage 'spring' independently. Jensen and Howell use mechanism theory to describe how compliant mechanisms that closely resemble four-bar linkages can exhibit bistability. They limit energy storage to strain energy, and they only consider compliant mechanisms with one major torsion spring. Therefore, their results shed very little insight into the true coupling of kinematics and forces that can be present in devices that have more range of motion or more than one energy storage element. Nevertheless, Jensen and Howell (2000) seem to be one of the few to attempt any sort of generalized design synthesis for non-buckling multistable systems.

Although there is some literature on the design of bistable mechanisms, the literature appears to lack any discussion of generalizing the idea to multiple (greater than two) equilibrium positions, particularly in systems that span multiple energy domains. Further, very little or no discussion is given to the restrictions and solution possibilities of the location of additional stable positions once the first one is specified. There is also a lack of discussion in terms of creating bistable or MSE systems with distinct natural frequencies or stiffnesses at each equilibrium position. In this work, we present a design synthesis methodology that will be a foundation for creating designs based on MSE systems that have multiple passive, but tailored, dynamic responses.

This article describes the design methodology for synthesis of MSE systems. Section 2 describes the general solution methodology including how to derive a performance index used for optimization. Section 3 describes an example linkage problem as a demonstration of the design synthesis methodology. Section 4 ends the article with descriptions of future work topics and conclusions.

## 2 General design synthesis methodology

### 2.1 Mathematical foundation of design synthesis methodology

To design an MSE system correctly, one needs a way to transfer qualitative and quantitative engineering characteristics to a meaningful mathematical form that is problem independent. We show that given the ability to model a system's energy, one can create a framework about which an MSE system can be designed. The design methodology focuses on using a potential energy of the system so that multiple energy domains (i.e. mechanical, electrical, magnetic, etc.) in any given system can all be taken into account.

To derive the system equations of motion about a stable equilibrium point, we start with defining the equilibrium point by (1) where $q$ is a general displacement, $\mathbf{p}$ is a vector of system design variables, and $V(q, \mathbf{p})$ is the system potential energy.

$$\left.\frac{\partial V(q, \mathbf{p})}{\partial q}\right|_{e_i} = 0\,, \quad i = 1, 2, \ldots n\,, \tag{1}$$

We then form the system Lagrangian in (2) with $(T(q, \dot{q}))$ as the system kinetic coenergy.

$$L(q, \dot{q}, \mathbf{p}) = T(q, \dot{q}, \mathbf{p}) - V(q, \mathbf{p}) = \frac{1}{2} m_{eff}(q, \mathbf{p}) \dot{q}^2 - V(q, \mathbf{p}) \tag{2}$$

By using the method of Lagrange, the equation of motion for an undamped and unforced single degree of freedom system is shown in (3).

$$0 = \frac{\mathrm{d}}{\mathrm{d}t}\left(\frac{\partial L(q, \dot{q}, \mathbf{p})}{\partial \dot{q}}\right) - \frac{\partial L(q, \dot{q}, \mathbf{p})}{\partial q} = m_{eff}(q, \mathbf{p})\ddot{q} + \frac{1}{2}\frac{\partial m_{eff}(q, \mathbf{p})}{\partial q}\dot{q}^2 + \frac{\partial V(q, \mathbf{p})}{\partial q} \tag{3}$$

For slowly varying and localized systems, a linearized model without the "$\dot{q}^2$" term is a reasonable approximation, as in (4), where $K_{eff,i}$ is the constant effective stiffness about equilibrium, $q_i$.

$$0 = m_{eff}(q_i, \mathbf{p})\ddot{q} + K_{eff,i}(q - q_i) \tag{4}$$

For stable equilibria $K_{eff,i} > 0$, and for unstable equilibria $K_{eff,i} < 0$ (Greenwood 1988). Using (4), the approximate natural frequency, $f$ (Hz), of the system at equilibrium $i$ is given by

$$f_i = \frac{1}{2\pi}\sqrt{\frac{K_{eff,i}}{m_{eff,i}}} \tag{5}$$

If describing an unstable equilibrium, (5) results in an imaginary number, and one must take account of this when optimizing so that the performance index decreases (or increases) properly.

In designing MSE systems, one must predefine desired shape characteristics of the energy curve and compare them to the candidate curve (see Fig. 1). From (4), the local linear generalized restoring force is $F(q) = K_{eff,i}(q - q_i)$ so that the potential energy of the localized mass-spring system is approximated as a quadratic equation:

$$V_i(q, \mathbf{p}) = \int F(q, \mathbf{p})\,\mathrm{d}q = \int K_{eff,i}(q - q_i)\,\mathrm{d}q = \frac{1}{2}K_{eff,i}(q - q_i)^2 + V_{nom,i} \tag{6}$$

where $V_{nom,i}$ is the value of energy at the equilibrium point. $K_{eff,i}$ accounts for all mechanical forces acting on the system with respect to coordinate $q$. Equation (6) shows the important quantities for the design engineer: $K_{eff,i}$, which relates to natural frequency, and $V_{nom,i}$, which relates to the energy required to move from one equilibrium to the next. Consider $q_i$ a stable equilibrium ($K_{eff,i} > 0$) and $q_j$ an adjacent unstable equilibrium ($K_{eff,i} < 0$) to be overcome. Then $\Delta V_{ij} = V_{nom,j} - V_{nom,i}$ provides a measure of stability as it is the required energy to move from $q_i$ to the next stable equilibrium.

### 2.2 Design synthesis process

Once the energy and effective inertia of the system are formulated as a function of the kinematic degrees of freedom,

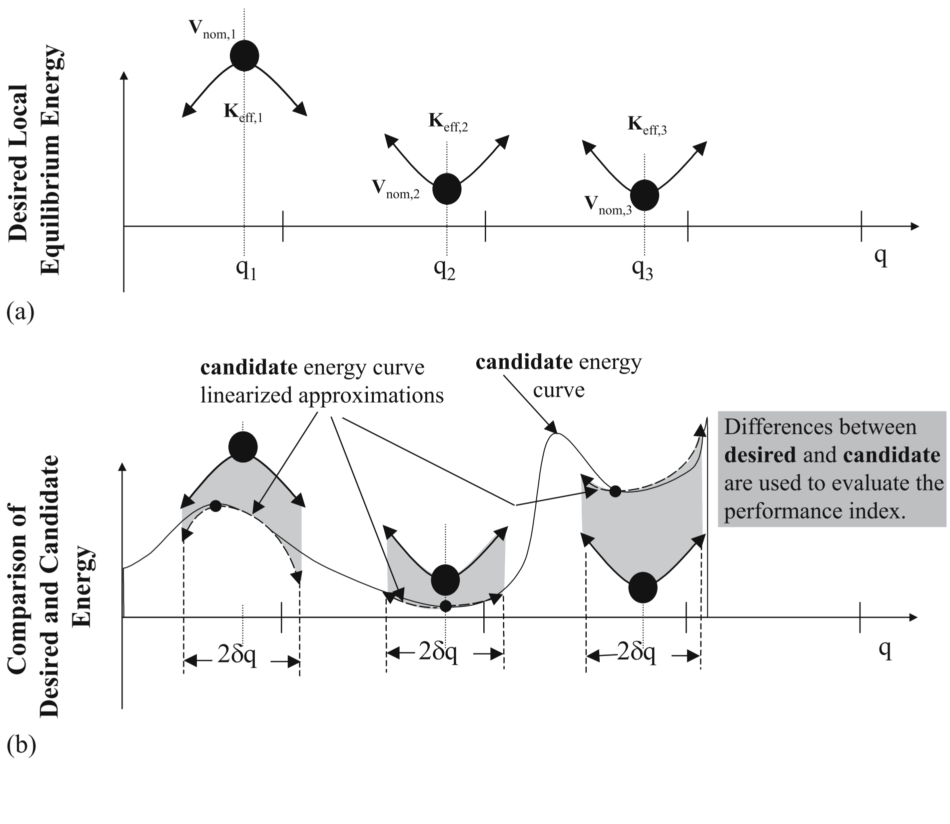


**Fig. 1** **a** The desired local equilibrium curve fit parameters. **b** Desired (solid) and candidate (dashed) quadratic curve fit approximations at the equilibrium points

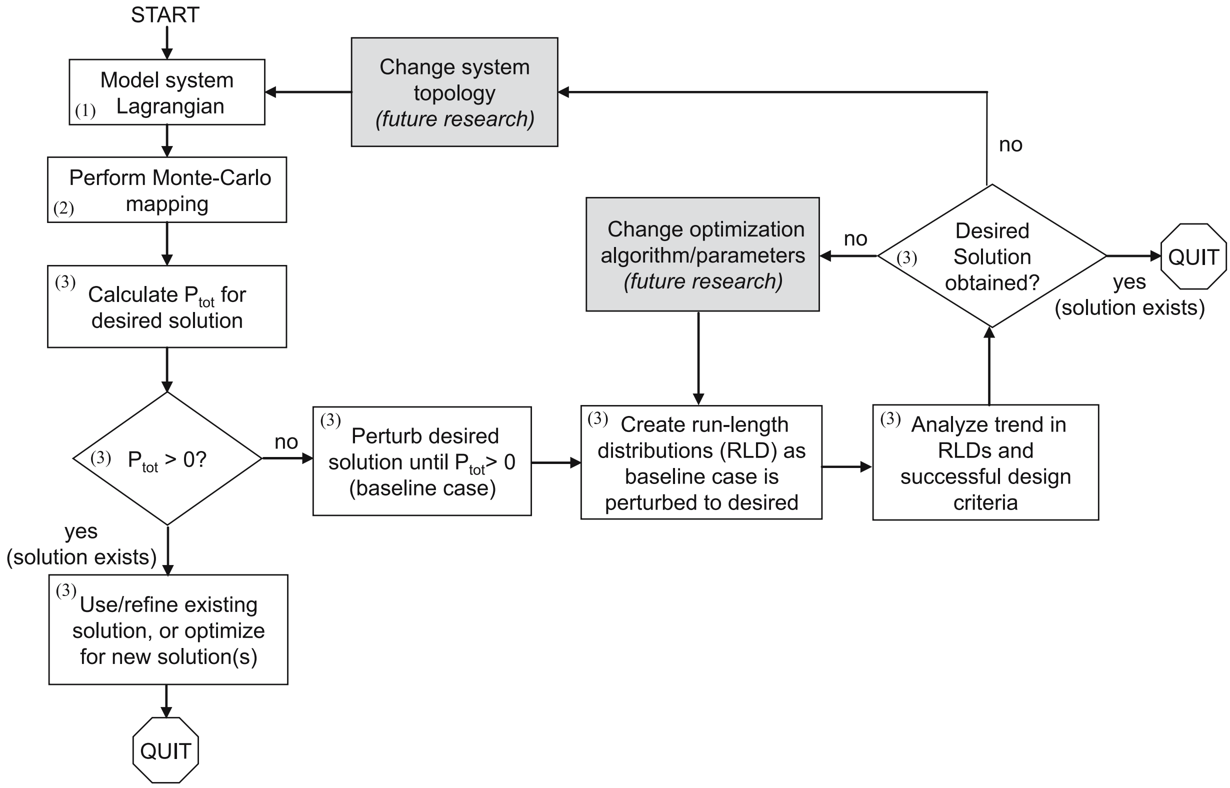


**Fig. 2** Flow chart designating the phases of the MSE design synthesis methodology. The design methodology phase numbers are shown in parentheses and discussed in detail in the following subsections

one can use the proposed design methodology to solve for the allowable MSE system characteristics as well as the unknown values for the design variables that are needed to produce the desired MSE system. When synthesizing an MSE system, a fundamental question arises: for a desired number of equilibrium positions with defined characteristics (i.e. natural frequency, energy value/difference), does a solution of the specified topology exist that meets the desired characteristics? Since the answer to this question is not intuitive, the design methodology is specifically created to help determine whether or not a solution exists. The existence of a solution means that it must meet all specifications. For instance, if one desires a tristable system, a bistable system will not suffice no matter how close the two candidate stable equilibrium positions are to any of the desired stable positions. To formulate the problem in this discrete fashion, we define an acceptable range, $\pm\delta$, about each desired design criterion. For each important design criterion, $q_i$, $f_i$ (or $K_{eff,i}$), and $V_{nom,i}$, an acceptable range should be specified such that, when each desired design criterion falls within its acceptable range, the total desired solution is considered to exist and be obtained.

The flow chart shown in Fig. 2 demonstrates the design methodology. There are three main phases, described in more detail in the following sections. Phase 1 is the modeling of the system energies, or ability to form the Lagrangian of (2). Phase 2 is the Monte Carlo mapping which acquires data to use as a baseline case for optimization and probability calculations. Phase 3 is an iterative process between optimization and probability calculation that allows the designer to know how well a particular algorithm is solving for the desired solution if it is not easily attainable. Thus, information is gathered about solution existence if the solution is not found easily, and the designer has some impetus for either abandoning the solution process or altering the desired design to one that does exist. In this regard, the problem of existence sets the methodology apart from many optimization problems since there is no way to know a priori if running an optimization is worth the effort.

### *2.2.1 Phase 1: modeling of system energy*

This phase is no more than assuring that one can formulate the Lagrangian of (2), which is needed to determine the location of the equilibrium positions and derive the effective mass of the system. These factors are used in the performance index of the optimization process.

### *2.2.2 Phase 2: Monte Carlo mapping*

The purpose of the Monte Carlo mapping is to give a baseline case for assessing feasibility of a desired MSE solution. This is helpful because of the nonintuitive nature of the problem. The data from the Monte Carlo process are then used in Phase 3 while optimizing.

The Monte Carlo mapping process is nothing more than cataloging the equilibrium position information that results from using a randomized set of design variables. The steps of the Monte Carlo process are as follows:

(i) Choose upper and lower bounds for each design variable
(ii) Randomly generate a set of design variables and evaluate the equilibrium characteristics of the system in terms of the equilibrium position and coefficients of (4)
(iii) Record data from Step (ii) and repeat several times.

*2.2.3 Phase 3: probability calculation and optimization*

This final design phase is the most extensive as it is the key to MSE design. It quantifies the Monte Carlo mapping method in a way that is not limited by the complexity of the problem in terms of number of stable equilibria or kinematic degrees of freedom. This is done with the use of cumulative distribution functions (CDF). By creating conditional CDFs for each design criterion, one can take their derivatives to create conditional probability density functions (PDF). With a conditional PDF for each design criterion, one integrates in a range about the desired values to quantify a total probability $P_{tot}$ of a solution being possible. This probability is a number that is related to the ease with which a numerical optimization routine can solve for the unknown design variables.

To describe the calculation of a probability, define the continuous CDF, $\mathrm{CDF}_X(b)$, of a random variable $X$ as follows:

$$\mathrm{CDF}_X(b) = P\left\{E_b^X\right\} = P\{X \leq b\} = \int_{-\infty}^{b} \mathrm{PDF}_X(z)\,\mathrm{d}z \qquad (7)$$

for all real values $b$ in the range $-\infty \leq b \leq \infty$ (Bowker and Lieberman 1972). In (7), $E_b^X$ is the event, or set of outcomes in the solution space, such that value of the random variable $X$ is less than or equal to the real number $b$, $P$ is the probability of such an event, and $\mathrm{PDF}_X(z)$ is the probability density function. As $b \to -\infty$, $\mathrm{CDF}_X(b) \to 0$, and if $\mathrm{PDF}_X(z) > 0$ for any number $b$, as $b \to \infty$, $\mathrm{CDF}_X(b) \to 1$.

Assume there are a total of $N$ data points generated during the Monte Carlo simulation. Some number $N_1$ of the data points have just one stable equilibrium position (event $E_{1eq}$), some number, $N_2$, have two stable equilibria (event $E_{2eq}$), and so on. For example, if designing a bistable MSE system, the first event used in calculating $P_{tot}$ is the event that there are two stable equilibria, $E_{2eq}$, with $N_2$ points of bistable data. Since this is a discrete condition, the probability that two equilibria occur is $P_{2eq} = N_2/N$.

In the case of multiple criteria, the total probability $P_{tot}$ for multiple equilibria and satisfaction of $m$ desired design criteria is found as a product of individual probabilities:

$$P_{tot} = P_{Meq} \prod_{i=1}^{m} P_i = P_{Meq} \prod_{i=1}^{m} \int_{lb_i}^{ub_i} \mathrm{PDF}_{X_i}(z)\,\mathrm{d}z \qquad (8)$$

In (8) $ub_i$ and $lb_i$ are the acceptable upper and lower bounds for the $i^{\text{th}}$ desired design criteria.

When optimizing, the performance index is simply a sum of penalty functions (Papalambros and Wilde 2000):

$$F = \sum_{i=1}^{m} \begin{cases} (d_{des,i} - \delta d_i) - d_{cand,i} & \text{if } d_{cand,i} < (d_{des,i} - \delta d_i) \\ d_{cand,i} - (d_{des,i} + \delta d_i) & \text{if } d_{cand,i} > (d_{des,i} + \delta d_i) \\ 0 & \text{otherwise} \end{cases} \qquad (9)$$

Here $m$ is the number of desired design criteria, $d_i$ is a dummy variable (substituting for $q_i$, $V_{nom,i}$, $f_i$, and $K_{eff,i}$) for the $i^{\text{th}}$ generic desired design criterion, and $\delta d_i$ is the acceptable tolerance on that criterion that is used in both optimization and the Monte Carlo probability calculation. There are two basic outcomes from the $P_{tot}$ calculation: $P_{tot} > 0$ and $P_{tot} = 0$. These are described in the following sections.

*Case 1: $P_{tot} > 0$*

If $P_{tot} > 0$ then this means that the desired solution is possible, or is known to exist, since it was found during the random sampling of the Monte Carlo mapping at least once. One can then use any of the solutions, refine those solutions, or optimize for the desired solution with a stochastic optimization algorithm. The number of iterations used in the Monte Carlo mapping can be used as an upper bound on iteration number for any intelligent, or guided, algorithm.

*Case 2: $P_{tot} = 0$*

Unlike in the case where $P_{tot} > 0$ we cannot immediately say anything about solution existence if $P_{tot} = 0$. There are two reasons why $P_{tot} = 0$ occurs: 1) not enough Monte Carlo data are present to represent the solution space fully, or 2) the solution does not exist. Distinguishing between these two scenarios is not straightforward, and the rest of the MSE design methodology attempts to give some confidence in whether or not the desired solution exists.

In analyzing the problem of solution existence for MSE systems, we use what we know about solution existence for $P_{tot} > 0$ and the concept of the run-length distribution (RLD). First, perturb the desired solution some amount $\delta\omega$ by slightly changing the properties of the desired design criteria until $P_{tot} > 0$ for this perturbed, or baseline, solution. This can mean changing the value of the desired criteria, i.e. change a desired equilibrium position from 1 to 2, or changing the acceptable upper and/or lower bounds $ub_i$ and $lb_i$ for one or more of the desired design criteria. The former changes the location of the desired solution in the performance space, and the latter relaxes the constraints on the problem.

With the baseline RLD in hand, we then optimize for MSE solutions as we reduce the perturbation distance, $\delta\omega$, from the baseline solution to zero. For each incremental solution as $\delta\omega$ decreases, we again create an RLD from some number of optimization runs. As solutions move toward and across the performance space boundary from a region of solution existence to a region of nonexistence, the RLD $\to 0$ showing that there is zero probability of solving the problem.

In optimizing the MSE problem, stochastic algorithms are used, thus the RLD is a representation of stochastic sampling much as the Monte Carlo data. The major difference is that the RLD data is guided by intelligent algorithms. Thus, if the calculated RLD $\to 0$ as $\delta\omega \to 0$ we still cannot prove that the solution does not exist. What we can approximate is how much time, or effort, is expected to solve for the true desired MSE solution. By tracking both the trends in the RLDs and the candidate design criteria as $\delta\omega \to 0$, we can gain a feeling for how close one is to the performance space boundary.

## 3 Demonstration problem

### 3.1 General problem description

The sample synthesis problem is that of a four-bar linkage with eight linear springs attached to the links of the mechanism (see Fig. 3). The linkage is assumed to be a Grashof mechanism, or Class I linkage, and therefore, the linkage construction is restricted such that the input crank (link $l_I$) can fully rotate 360° (Erdman and Sandor 2001). The linear translational springs are the only energy storage elements. Although the springs are linear, the linkage provides the nonlinear motion that enables multiple stable equilibria. Kinematically, this is a one degree of freedom system described by the input crank angle $\theta$.

The goal of the synthesis problem is to determine a combination of the following design variables: the spring constants ($k_i$) and free lengths ($lo_i$) of the eight springs, the locations of anchors for the springs fixed to the ground ($x_1, x_2, y_1, y_2$), and link lengths ($l_I$, $l_{II}$, $l_{III}$, $l_{IV}$). These variables will be optimized for an MSE system with desired locations ($\theta$) for each equilibrium position (stable or unstable) as well as other equilibrium properties.

More formally, a description of the synthesis problem is to design the MSE linkage system to meet any combination of the following objectives:

1. Stable equilibrium at $\theta_n$, $n = 1, 2, \ldots$
2. Frequency $f_n$ or $K_{eff,n}$ at stable equilibrium $\theta_n$, $n = 1, 2, \ldots$
3. Unstable equilibrium at $\theta_m$, $m = 1, 2, \ldots$
4. $K_{eff,m}$ at unstable equilibrium $\theta_m$, $m = 1, 2, \ldots$
5. Energy difference between equilibria, $\Delta V_{nm} = V_{stable,n} - V_{unstable,m}$, $n, m = 1, 2, \ldots$

### 3.2 Problem description

The design problem where variable link lengths are allowed corresponds to a scenario in which one is more interested in the frequency, stiffness, and energy value of each equilibrium, but not absolute position. Because the links can achieve various lengths during optimization, the coupler curve of the linkage varies, and thus must be irrelevant to the design. Nonetheless, one may want to attach this type of MSE system to another system simply to alter its performance or make it have multiple stable positions with certain natural frequencies.

Because absolute position of the linkage is not fixed, a solution approach is to design the relative distances between the equilibrium points. For example, if one wants two stable equilibria to be two radians apart, then this idea can be incorporated into the performance index. The same concept is applied to actuation energy (or $V_{nom}$ values) as well.

In order to evaluate (9), the equilibrium points must be found at each iteration by a line search along the energy curve. The $\theta_i$ (equilibria), $K_{eff,i}$, $f_i$, and $V_{nom,i}$ values are then calculated by performing a second-order curve fit about these equilibrium locations and equating the curve fitting coefficients to those of (6). Also, there is no guarantee that the correct number of equilibria will be present for any given iteration. A penalty factor is incorporated into the performance index if this occurs.

We assume the links have a fixed mass per unit length and an inertia that is only a function of link length. The problem statement then is as follows:

min $F(k_i, lo_i, x_1, x_2, y_1, y_2, l_I, l_{II}, l_{III}, l_{IV})$ $i = 1, 2, \ldots, 8$
s.t.

| | |
|---|---|
| 1. $k_i, lo_i \geq 0$, | – Spring constants and free lengths positive |
| 2. $k_i < k_{max}$, | – Spring constants below some maximum |
| 3. $lo_i < lo_{max}$, | – Free lengths below some maximum |
| 4. $x_1 < \mathrm{d}x_{max}$, | – Point $x_1$ less than some maximum |
| 5. $x_2 < l_{IV} + \mathrm{d}x_{max}$, | – Point $x_2$ less than some maximum |
| 6. $x_1 > -\mathrm{d}x_{max}$, | – Point $x_1$ greater than some minimum |
| 7. $x_2 > l_{IV} - \mathrm{d}x_{max}$, | – Point $x_2$ less than some minimum |
| 8. $y_i > -\mathrm{d}y_{max}$, | – Point $y_i$ greater than some minimum, $i = 1, 2$ |
| 9. $y_i < \mathrm{d}y_{max}$, | – Point $y_i$ less than some maximum, $i = 1, 2$ |
| 10. $l_I, l_{II}, l_{III}, l_{IV} < l_{max}$, | – Link lengths less than some maximum |
| 11. $l_I, l_{II}, l_{III}, l_{IV} > l_{min}$, | – Link lengths greater than some minimum |
| 12. $l_I < l_{II}, l_I < l_{III}, l_I < l_{IV}$, | – Input crank must be smallest |
| 13. $s + l < p + q$, | – Grashof Criterion ($s$-shortest link, $l$-longest link, $p$ and $q$ are other two links) |

#### 3.2.1 Phase 1: modeling of system energy

The Lagrangian of the system is:

$$L\left(\theta, \dot{\theta}, \mathbf{p}\right) = T\left(\theta, \dot{\theta}, \mathbf{p}\right) - V(\theta, \mathbf{p}) \tag{10}$$

where the potential energy is the summation of the eight spring energies:

$$V(\theta, \mathbf{p}) = \sum_{i=1}^{8} \frac{1}{2} k_i \left(l_i(\theta, \mathbf{p}) - lo_i\right)^2 \tag{11}$$

and the kinetic coenergy includes the linear and rotational inertias of the three moving links:

$$T\left(\theta, \dot{\theta}, \mathbf{p}\right) = \sum_{i=1}^{3} \frac{1}{2} m_i \left(\dot{x}_{gi}^2 + \dot{y}_{gi}^2\right) + \sum_{i=1}^{3} \frac{1}{2} I_{gi}\, \dot{\theta}_{gi}^2 \tag{12}$$

where $l_i(\theta, \mathbf{p})$ is the length of the $i^{\text{th}}$ spring as a function of $\theta$ and design vector $\mathbf{p}$. Further, $(x_{gi}, y_{gi})$ are the coordinates of the center of mass, $I_{gi}$ is the mass moment of inertia about the center of mass, and $\theta_i$ is the angular position of link $i$, respectively. Writing out the full expression for the system Lagrangian as an explicit function of $\theta$ involves many trigonometric functions needed to determine the link positions of a four-bar linkage (Erdman and Sandor 2001). Solving (10)–(12) to meet the constraints of (1) and desired properties of (4) is quite unwieldy, especially adding in the desired frequencies and acceptable ranges about each desired design criterion. Therefore, we employ the aforementioned MSE design methodology that uses the system energies for design.

### *3.2.2 Phase 2: Monte Carlo mapping*

The Monte Carlo mapping was performed with 49,541 data sets. The allowed ranges for the design variables were fixed by the following upper limits: $k_{max} = 3$ N/m, $lo_{max} = 2$ m, $dx_{max} = dy_{max} = 0.75$ m, $l_{max} = 2$ m, $l_{min} = 0.1$ m. The results produced 43,159 monostable designs, 5413 bistable designs, 955 tristable designs, and 14 quadrastable designs.

### *3.2.3 Phase 3: probability calculation and optimization*

*Bifurcating nature of the linkage problem*

Figure 4 shows the inherent nature of the optimization problem by plotting the length of a typical spring as a function of input crank angle, $\theta$. If this is the only spring in the system, the equilibria reside where $lo$ is closest to the actual spring length. In other words, the energy in the system is $V(\theta, k, lo) = (1/2)k(l(\theta) - lo)^2$, and this energy is minimized/maximized when $dV/d\theta = k(l(\theta) - lo)(dl(\theta)/d\theta) = 0$. Thus, if for any $\theta$ we obtain $lo = l(\theta)$, then that $\theta$ represents a stable position. If the condition $lo = l(\theta)$ is not met, then the equilibria lie at those $\theta$ where $dl(\theta)/d\theta = 0$, i.e. the spring reaches a minimal or maximal length.

In Fig. 4, one can see that, as $lo$ increases, the stable equilibria bifurcate from one region to the next. In Region I we have $lo \neq l(\theta)$ and the stable equilibrium is $\theta_I = 40°$ where $dl(\theta)/d\theta = 0$. Then, in Region II, $lo_{crit,1} < lo < lo_{crit,2}$, the condition $lo = l(\theta)$ is met twice. Finally, when $lo > lo_{crit,2}$ in Region III, the two stable equilibria merge back into only one stable equilibrium at $\theta_{eq,III} = 185°$ given by $dl(\theta)/d\theta = 0$. This bifurcating nature of the linkage problem poses inherent difficulties for gradient-based optimization methods which do not have strategies in place to handle multimodal spaces. For this reason, the problem necessitates some level of a stochastic or non-derivative-based optimization approach. We have chosen to use a genetic algorithm, although simulated annealing has also been shown to work well (Houck et al.; Ingber 1989).

*Optimization of the linkage problem*

With the problem now fully defined, we create the set of desired design criteria:

1. Bistable system
2. $\theta_{des,2} - \theta_{des,1} = 3.2 \pm 0.05$ radians (difference between stable equilibria)
3. $f_1 = f_2 = 0.16 \pm 0.03$ Hz
4. $\Delta V_{21} = \Delta V_{22} = 0.25 \pm 0.2$ J (energy hump about $\theta_2$)
5. Find maximum $\Delta V_{11} = \Delta V_{12}$ (energy hump about $\theta_1$).

The values of $P_{tot}$ were calculated from the mapping data for the desired designs as they are perturbed in several incremental cases. We start with the baseline design (call it Case 1), with $\Delta V_{11} = V_{1,unstable} - V_{1,stable} = V_{2,unstable} -$

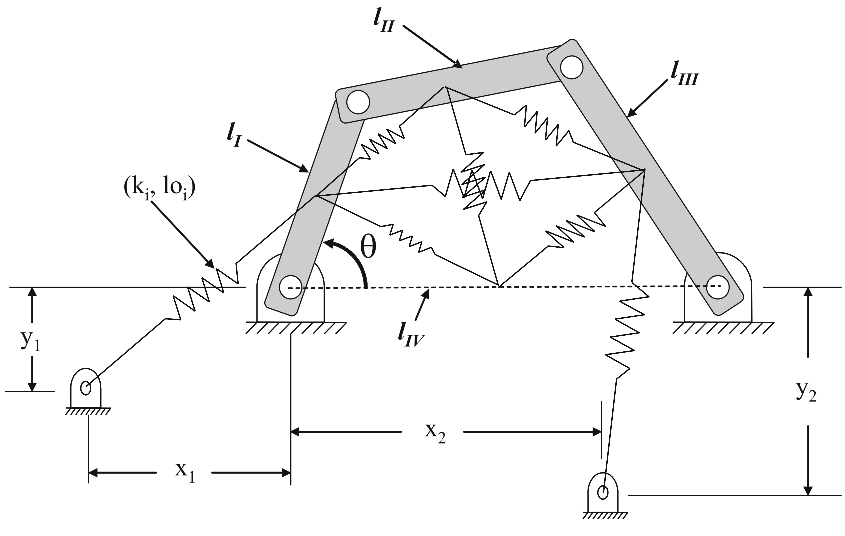


**Fig. 3** Four-bar linkage demonstration problem

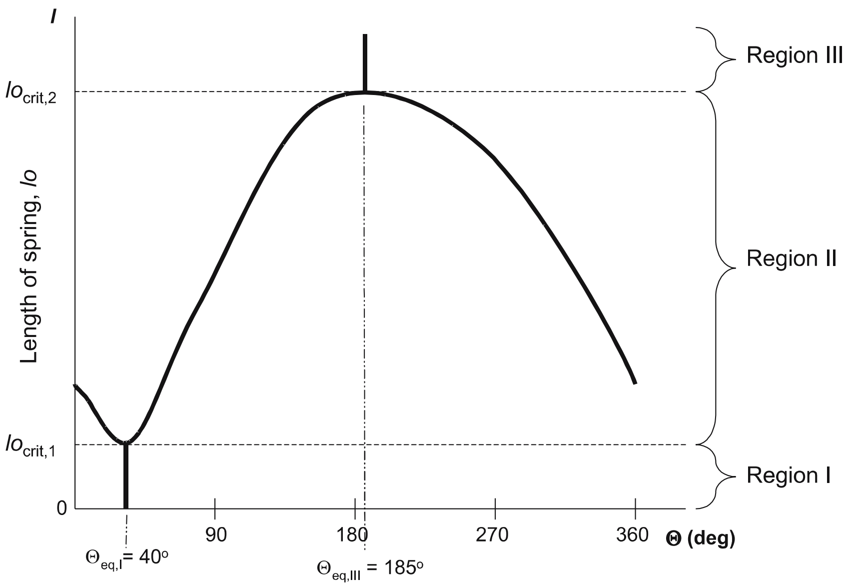


**Fig. 4** Plot of the spring length versus $\theta$ shows how the spring length can determine stable equilibria

$V_{1,stable} = 1.0 \pm 0.2$ J, since it has $P_{tot} > 0$, with $P_{tot} = 3.7 \times 10^{-5}$. All other Cases 2–23 vary $\Delta V_{11}$ in increments of $\delta\omega = 1.0$ J up to the value of 23 J for Case 23 as we try to find the perceivable limit of $\Delta V_{11} = \Delta V_{12}$. All Cases 2–23 have $P_{tot} = 0$.

The baseline solution is one that is 1) known to exist, 2) similar in scope to the true desired solution (i.e. has same number of equilibria and the same number and type of design criteria), and 3) is relatively close to the true desired solution. Therefore, by optimizing for this baseline solution, say $r$ times, with a given algorithm, we can arrange the resulting data of these $r$ optimization runs to provide a baseline run-length distribution (RLD). The RLD is a CDF of the number of iterations required to solve for a desired MSE

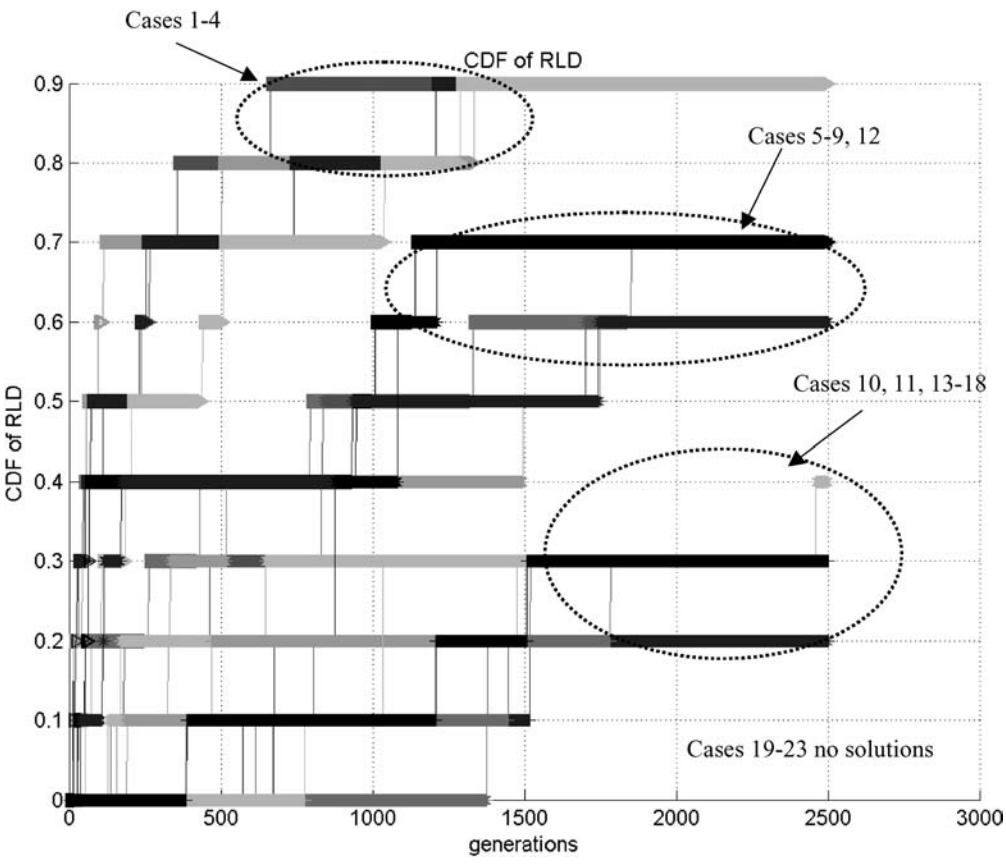


**Fig. 5** The run-length distribution as the desired solution is perturbed

design (Stützle and Hoos 1999). The baseline case thus provides a way to see how quickly a chosen algorithm solves for a solution known to exist so we can assess the ability of the algorithm to solve for desired solutions that are not known to exist.

The RLD for solving the linkage problem is created using 10 trials for each desired solution, a genetic population of 100 individuals, and a limit of 2500 generations (see Fig. 5). Note how even Case 1 is not solved every time within the 2500 generations as only 9 out of 10 trials are solved successfully. Cases 2–4 are solved with similar ease compared to the baseline case.

Figure 5 shows three basic groups of solutions: 1) Cases 1–4 that are solved nearly every time, 2) Cases 5–18 that are solved in 20%–70% of the trials, and 3) Cases 19–23 that were not solved in any of the trials. Certainly not solving Cases 19–23 in any of the 10 trials does not prove that those solutions are nonexistent. On the other hand, the trend of the RLD certainly shows an increased difficulty in moving away from the baseline case solution. If spending more time is warranted in solving for Cases 19–23, we have the options of tweaking the genetic algorithm parameters, running the algorithm for more generations, or using a different optimization algorithm.

To explore the apparent approach to a performance space boundary more fully, we plot the locations of the equilibrium positions to observe any limiting trends as we perturb from the baseline case. Figure 6a shows the energy hump values, $\Delta V_{11} = \Delta V_{12}$, as they are perturbed, and Fig. 6b shows the equilibrium positions, stable and unstable, as the desired solution is perturbed moving to the right. Dots represent stable equilibrium positions, and crosses represent unstable equilibria.

Notice two major groups of solutions, dictated by the dotted and dashed lines that encircle the stable equilibria of Fig. 6b. We know they are solutions in separate regions of the performance space since the stable equilibrium positions are supposed to be $3.2 \pm 0.2$ radians apart. Thus, the solutions in the dashed circle for $\theta_{eq,1}$ can only be associated with the solutions in the dashed circle for $\theta_{eq,2}$.

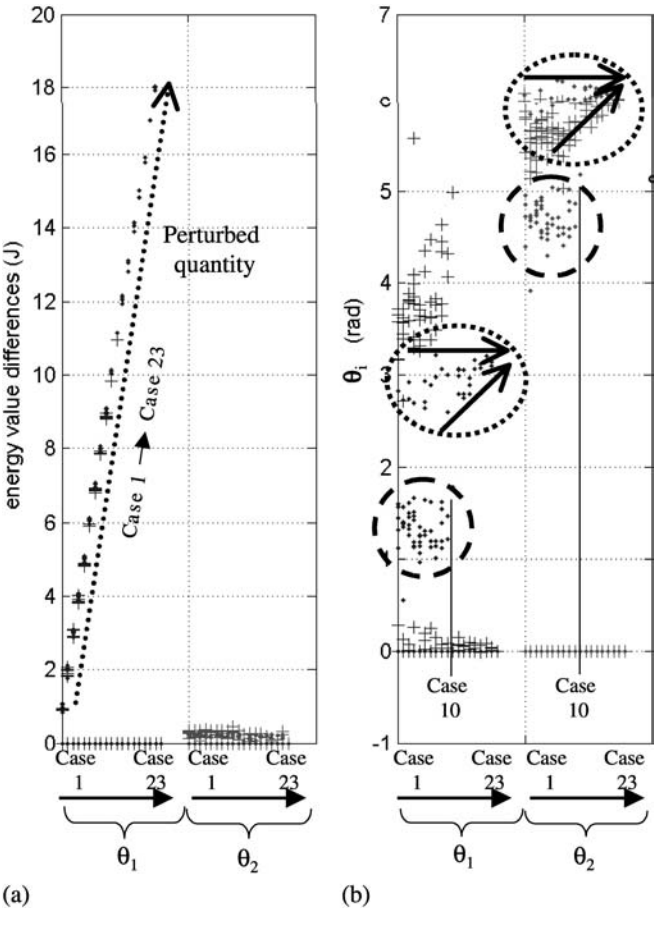


**Fig. 6** Trends in the **a** energy hump values and **b** equilibrium positions as the desired solution is perturbed from the baseline case. Dots represent stable equilibrium positions, and crosses represent unstable equilibrium positions

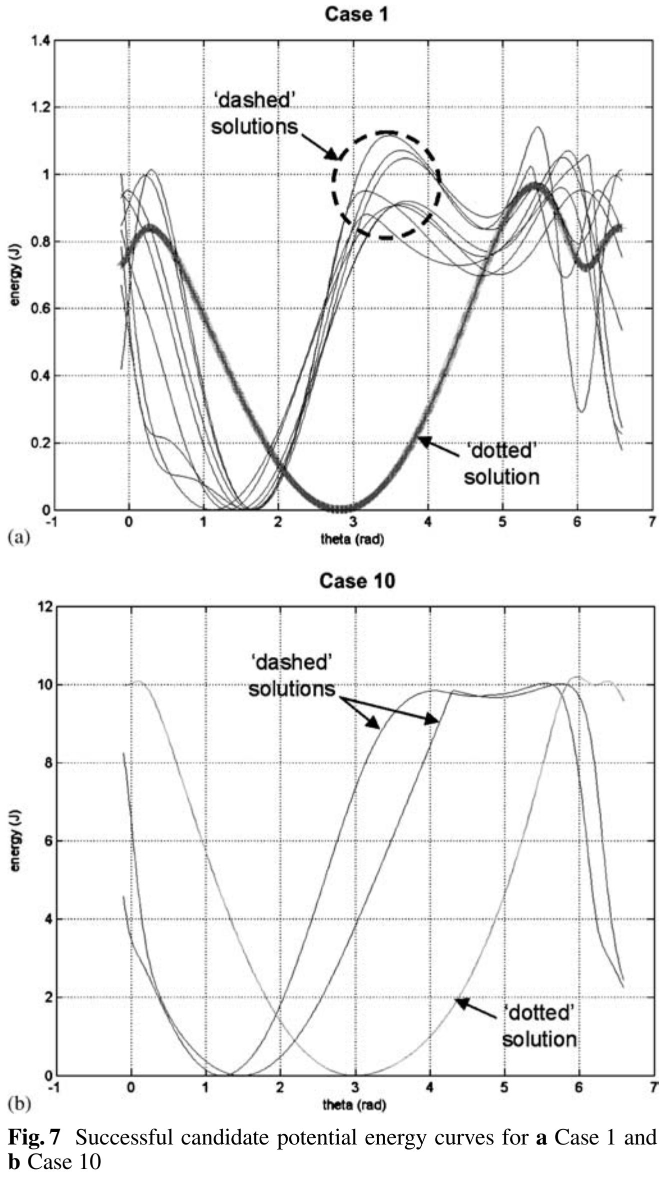


**Fig. 7** Successful candidate potential energy curves for **a** Case 1 and **b** Case 10

Figure 6b shows that after Case 10 the solutions in the dashed circle no longer appear. After Case 10, the acceptable performance space is shown only by solutions in the dotted circles. As shown by the arrows, the equilibrium positions in the dotted circles show a contracting trend where the acceptable values occur as the solution is perturbed past Case 10. This range where the equilibrium positions are found decreases until it becomes zero at Case 19 where there are no solutions.

Figure 7a shows the energy curves for Case 1 and Fig. 7b for Case 10. One can see the two fundamentally different energy curve shapes that were found in different regions of the performance space. Two of the energy curves in Fig. 7a are actually tristable designs. Since the performance index only calculated the first two equilibrium positions, the third one did not malign the ranking of the design.

Figures 6 and 7 lend credence to the idea that as the desired solution gets perturbed further from the baseline case, the desired solution leaves the feasible performance space. This concept is intuitive, but what is not clear is exactly how far one must perturb the system to reach this solution space boundary. By using the RLD and tracking the results of several optimization runs, we can begin to define where this boundary region lies. In the example problem, the performance space boundary lies near to where $\Delta V_{11} = \Delta V_{12} = 19.0 \pm 0.2$ J, where solutions were proven to exist for $\Delta V_{11} = \Delta V_{12} \leq 18.0 \pm 0.2$ J.

Defining this boundary is a crucial activity for the MSE designer. He ideally would like to determine if the set of parameters can make a certain topology achieve an MSE design goal. Given ample search time, optimization can find such a solution if one exists. However, our MSE design approach also predicts if such an optimization is a worthy effort.

## 4 Conclusions and future work

In this paper we describe a design synthesis methodology for multistable equilibrium systems. The phased design process begins by modeling the system with standard Lagrangian methods and then uses a Monte Carlo mapping technique together with numerical optimization algorithms to solve for unknown design variables. The design approach is based upon linearizing the Lagrangian about each local equilibrium. The coefficients of this linearized curve systematically relate to the three major design criteria used to describe equilibrium points: equilibrium location, energy value, and energy stiffness (the last is directly relates to natural frequency). A mapping method involving probability calculations enables a beginning quantification of achievable values for these design criteria.

The method is general enough to account for any number of equilibria in a system that stores potential energy. By the example of the four-bar linkage problem we have shown how to use the design methodology to design for a few basic traits of an MSE system: equilibrium position, localized natural frequency at each stable equilibrium, and difference in energy between stable and unstable equilibria (actuation energy).

One benefit of our solution approach using only the system Lagrangian is that it applies to other problems where the mathematics becomes difficult. Such scenarios include problems in which there is either no closed form for the potential energy (such as being derived from a continuous field using finite elements) or unknown kinematics of the system. An example is in fully coupled multiple energy domain problems such as compliant structures.

This paper describes a foray into the design of MSE systems. Future work in this area can focus on many parts of the design methodology. In the Monte Carlo mappings used in this paper, on the order of $10^4$ iterations were run, but more work needs to be done to determine how many iterations are necessary. Additional work in the topological assessment of problems needs to be addressed, including compliant structures. For instance, the example problem assumes that all springs are necessary. A topological assessment could begin to explore what types and how many energy storage elements (i.e. springs, magnetic fields, etc.) are needed in a design.

**Acknowledgement** The authors would like to thank the National Science Foundation for supporting this work under grant award number CMS-0201433.

## References

Capanu M, Boyd JG, Hesketh PJ (2000) Design, fabrication, and testing of a bistable electromagnetically actuated microvalve. J Microelectromech Syst 9(2):181–189

Chironis NP (1991) Mechanisms and mechanical devices sourcebook. McGraw-Hill, New York

Erdman AG, Sandor GN, Kota S (2001) Mechanism design: analysis and synthesis, Vol. 1. 4th edn. Prentice-Hall, NJ

Greenwood DT (1988) Principles of dynamics. 2nd end. Prentice-Hall, New Jersey,

Hafez M, Lichter MD, Dubowsky S (2002) Optimized binary modular reconfigurable robotic devices. Proceedings of the 2002 IEEE International Conference on Robotics and Automation, Washington D.C.

Hoffman M, Kopka P, Voges E (1999) Bistable micromechanical fiber-optic switches on silicon with thermal actuators. Sens and Actuators 78:28–35

Houck CR, Joines, JA, Kay MG (1995) A genetic algorithm for function optimization: a matlab implementation. North Carolina State University

Howell LL, Rao SS, Midha A (1994) Reliability-based optimal design of a bistable compliant mechanism. J Mech Des 116:1115–1121

Ingber AL (1989) Very fast simulated re-annealing. J Mathl Comput Model 12:967–973

Jensen BD, Howell LL (2000) Identification of compliant pseudo-rigid-body mechanism configurations resulting in bistable behavior. The Proceedings of the 2000 ASME Design Engineering Technical Conference, Baltimore, Maryland, Paper No. DETC2000/MECH-14147

Jensen BD, Howell LL, Salmon LG (1998) Introduction of two-link, in-plane, bistable compliant MEMS. The Proceedings of the 1998 ASME Design Engineering Technical Conference, Atlanta, Georgia, Paper No. DETC98/MECH-5837

Opdahl PG, Jensen BD, Howell LL (1998) An investigation into compliant bistable mechanisms. The Proceedings of the 1998 ASME Design Engineering Technical Conference, Atlanta, Georgia, Paper No. DETC98/MECH-5914

Papalambros P, Wilde D (2000) Principles of optimal design: modeling and computation. 2nd edn. Cambridge University Press
Pfaffenberger RC, Patterson JH (1987) Statistical methods: for business and economics, 3rd edn. Richard D. Irwin
Saif M, Taher A (2000) On a tunable bistable MEMS — theory and experiment. J Microelectricalmech Syst 9(2):157–170
Schomburg WK, Goll C (1998) Design optimization of bistable microdiaphragm valves. Sens Actuators A 64:259–264
Schulze EF (1955) Designing snap-action toggles. Prod Eng 26(1):168–170
Stützle T, Hoos HH (1999) Analyzing the run-time behaviour of iterated local search for the TSP. Proceedings of the 1999 Metaheuristics International Conference, Angra dos Reis, Brazil, July 19–22
Vangbo M, Bäcklund Y (1998) A lateral symmetrically bistable buckled beam. J Micromech Microeng 8:29–32